Journal of Power Sources 190 (2009) 271–278

Contents lists available at ScienceDirect

Journal of Power Sources

journal homepage: www.elsevier.com/locate/jpowsour

The use of stainless steel and nickel alloys as low-cost cathodes in microbial electrolysis cells

Priscilla A. Selembo[a,1], Mathew D. Merrill[b,1], Bruce E. Logan[b,*]

[a] Department of Chemical Engineering, Pennsylvania State University, University Park, PA 16802, USA
[b] Department of Civil and Environmental Engineering, Pennsylvania State University, 212 Sackett Building, University Park, PA 16802, USA

ARTICLE INFO

Article history:
Received 4 December 2008
Received in revised form
23 December 2008
Accepted 24 December 2008
Available online 17 January 2009

Keywords:
BEAMR
MEC
Electrohydrogenesis
Hydrogen production
Metal cathode
Stainless steel
Nickel

ABSTRACT

Microbial electrolysis cells (MECs) are used to produce hydrogen gas from the current generated by bacteria, but low-cost alternatives are needed to typical cathode materials (carbon cloth, platinum and Nafion™). Stainless steel A286 was superior to platinum sheet metal in terms of cathodic hydrogen recovery (61% vs. 47%), overall energy recovery (46% vs. 35%), and maximum volumetric hydrogen production rate (1.5 $m^3\ m^{-3}\ day^{-1}$ vs. 0.68 $m^3\ m^{-3}\ day^{-1}$) at an applied voltage of 0.9 V. Nickel 625 was better than other nickel alloys, but it did not perform as well as SS A625. The relative ranking of these materials in MEC tests was in agreement with cyclic voltammetry studies. Performance of the stainless steel and nickel cathodes was further increased, even at a lower applied voltage (0.6 V), by electrodepositing a nickel oxide layer onto the sheet metal (cathodic hydrogen recovery, 52%, overall energy recovery, 48%; maximum volumetric hydrogen production rate, 0.76 $m^3\ m^{-3}\ day^{-1}$). However, performance of the nickel oxide cathodes decreased over time due to a reduction in mechanical stability of the oxides (based on SEM–EDS analysis). These results demonstrate that non-precious metal cathodes can be used in MECs to achieve hydrogen gas production rates better than those obtained with platinum.

1. Introduction

Electrohydrogenesis is a promising process to produce hydrogen gas from organic matter in devices known as microbial electrolysis cells (MECs) [1]. In an MEC, exoelectrogenic bacteria oxidize organic matter, which generate CO_2, electrons and protons. The bacteria transfer the electrons to the anode and the protons are released to the solution. By adding a small voltage to that produced by the bacteria (~0.2 V) to overcome the endothermic barrier of hydrogen formation (−0.414 V for acetate), electrons and protons are catalyzed at the cathode to form hydrogen gas. Typically voltages of ~0.3 V or larger are needed to overcome electrode overpotentials. This electrical input is less than the voltages required for water electrolysis (typically 1.8–2.0 V) [1]. MECs are especially useful when the organic matter used in the process originates from wastewater or non-food biomass sources such as corn stover.

While MEC tests have so far been limited to the laboratory, these reactors will need to be scaled-up to sizes suitable for real-world applications [2]. One of the challenges of scaling up MECs is the cost of the cathode and the cathode catalyst. Most MECs use platinum applied to carbon cloth [3–5] or carbon paper [6,7] using a binder (i.e. Nafion™), but both the carbon cloth and the binder are expensive. Therefore, it is necessary to identify other cathode materials for this MEC technology to be economical.

There have been very few investigations into alternative cathode materials for MECs. Comparisons of the performance of cathode materials among studies can be difficult as the system conditions and architecture also affect reactor performance. Titanium mesh with platinum catalyst [8,9] has been used in two-chamber and one-chamber (with membrane) configurations, but hydrogen production rates were low (up to 0.3 $L\ L^{-1}\ day^{-1}$ at 1.0 V applied voltage). A combination of palladium and platinum catalyst on carbon paper [10] was used in a continuous flow reactor, but this system produced high concentrations of methane. In another study, it was observed that hydrogen evolution could be catalyzed using only bacteria on a plain electrode (graphite felt), referred to as a biocathode [11]. The best results have been achieved using a single-chamber MEC with acetate as a substrate and platinum on carbon cloth cathodes. At an applied voltage of 0.8 V, for example, hydrogen was produced at a maximum volumetric production rate of $Q = 3.12\ m^3\ m^{-3}\ day^{-1}$, with a cathodic hydrogen recovery $r_{H_2,cat} = 96\%$ and an overall energy efficiency of $\eta_{E+S} = 75\%$ [3]. In contrast, the two-chamber MEC with a biocathode [11], operated at an applied voltage of 0.7 V under continuous flow conditions,

* Corresponding author. Tel.: +1 814 863 7908; fax: +1 814 863 7304.
E-mail addresses: pag8@psu.edu (P.A. Selembo), merrill@engr.psu.edu (M.D. Merrill), blogan@psu.edu (B.E. Logan).
[1] Tel.: +1 814 865 9387; fax: +1 814 863 7304.

0378-7753/$ – see front matter © 2009 Elsevier B.V. All rights reserved.
doi:10.1016/j.jpowsour.2008.12.144

Table 1
Stainless steel and nickel alloys composition (% by weight).

Alloy	Fe	C	Mn	P	S	Mo	Si	Cr	Ni	Cu	Other	Other
SS 304		0.08	2	0.45	0.03	0	1	18–20	8–10.5	1		
SS 316		0.08	2	0.05	0.03	2–3	1	16–18	10–14	2–3		
SS 420		0.15	1	0.04	0.03	0	1	13				
SS A286		0.08	2	0.025	0.025	1–1.5	1	13.5–16	24–27		1.9–2.35 Ti	
Ni 201	0.4	0.02	0.35						99	0.25	0.35 Si	0.01 S
Ni 400	1.6		1.1						65.1	32		
Ni 625	2.5					9		21.5	61		3.6 Nb	
Ni HX	18	0.1				9		22	47		0.6 W	1.5 Co

produced a gas flowrate of $Q = 0.63\ m^3\ m^{-3}\ day^{-1}$ and a cathodic hydrogen recovery of $r_{H_2,cat} = 49\%$.

Various metals have been examined for use in water electrolyzers to catalyze the hydrogen evolution reaction (HER) [12]. First row transition metals are desirable as they are stable, abundant in nature, economical, and have low toxicity to living organisms. The most promising materials identified so far are nickel and stainless steel alloys based on cost, availability, low overpotentials, and stability in solutions which are usually highly alkaline. A comparison of stainless steel alloys (304, 316 and 430) in an alkaline electrohydrolyzer showed that SS 316 was the best of these three materials for HER [13]. In another study, SS 310 was compared to Raney nickel alloys in a commercial electrolyser [14], and it was concluded that the use of SS 310 would theoretically make the system 16 times cheaper at similar hydrogen production rates. Nickel alloys SAF 2205, INCONEL 625 and MONEL 400 were evaluated for hydrogen evolution using cyclic voltammetry [15]. SAF 2205 showed more favorable overpotentials for HER in 1 M NaOH than carbon steel SAE1020. Nickel oxide catalysts also have shown great promise as catalysts for hydrogen evolution [16] by water electrolysis under alkaline conditions. The main limitation in extending the previous results with these metals to MECs is that they have only been examined using highly alkaline conditions. MECs operate at near-neutral pH, and thus the efficacy for hydrogen evolution of nickel and stainless steel materials under these conditions have not been evaluated with respect to more conventional catalysts such as platinum.

In this study, different nickel and stainless steel alloys were compared under neutral pH conditions to platinum using sheet metal cathodes in MECs. Most MECs use particles of the catalyst bound to highly porous carbon cloth. Under these conditions, catalyst particle size, binding efficiency, and other factors can influence current densities. A baseline comparison of these different metals was therefore made here using flat surfaces to remove variability of the materials based on surface area and binders. The performance of two of these materials was also examined with a nickel oxide deposited onto the sheet metal surface. For comparison with typical MEC cathodes, we also conducted MEC tests using platinum bound to a carbon cloth cathode.

2. Materials and methods

2.1. MEC reactor construction

Single-chamber MEC reactors consisted of 4 cm long by 3 cm diameter cylindrical chambers formed from a solid block of Lexan, as described by Call and Logan [3]. The anodes were ammonia treated graphite brushes (25 mm diameter × 25 mm length, 0.22 m^2 surface area) [17,18]. Reactors were inoculated with the anode solution from another acetate-fed MFC reactor that had been running for over 1 year using acetate ($1\ g\ L^{-1}$) and a phosphate buffer nutrient medium [18]. The inoculum was omitted once a reactor produced >0.3 $mA\ cm^{-2}$. The medium consisted of a 50-mM phosphate buffer solution ($4.58\ g\ L^{-1}$ Na_2HPO_4 and $2.45\ g\ L^{-1}$ $NaH_2PO_4{\cdot}H_2O$; pH 7.0), $0.31\ g\ L^{-1}$ NH_4Cl, $0.13\ g\ L^{-1}$ KCl, and trace vitamins and minerals [19]. MECs were operated in fed-batch mode. A power source (3645A; Circuit Specialists, Inc., AZ) was used to apply either 0.6 or 0.9 V to the reactors. After each cycle, the reactors were drained, refilled with substrate solution, and sparged with ultra high purity nitrogen gas for 5 min. The reactors were maintained in a 30-°C constant temperature room. Once reactors reached similar current (~0.57 $mA\ cm^{-2}$) and gas production volumes (~30 ml) for three consecutive cycles using carbon cloth cathodes, the cathodes were replaced with sheet metal cathodes. All reactors were run in duplicate, and tests with new cathodes were run for at least three consecutive cycles.

2.2. Cathodes

Stainless steel alloys 304, 316, 420 and A286 and nickel alloys 201, 400, 625 and HX were made by cutting sheet metal (McMaster-Carr, IL) into 3.8 cm diameter disks. Metal compositions are listed in Table 1. A platinum metal disk (99.9% purity) used for comparison to these other metal materials was pre-cut by the manufacturer (Hauser & Miller, MO). Metal cathodes were cleaned with ethanol before placing them in the reactors. Carbon cloth cathodes (projected surface area of 7 cm^2) were made using a platinum catalyst ($0.5\ mg\ cm^{-2}$) and a Nafion binder, with the catalyst layer facing the anode [20].

2.3. Nickel oxide electrodeposition

The nickel oxide catalyst was created through cathodic electrodeposition onto a sheet metal support [16] using a 12.9-cm^2 nickel foam anode. Electrodeposition was achieved by applying 20 V at ~2 A for 30 s (1696 power source, B&K Precision, CA) in a solution containing 12 mM $NiSO_4$ and 20 mM $(NH_4)_2SO_4$ at a pH 2.0, adjusted by adding H_2SO_4. Cyclic voltammetry (CV) scans were performed on the electrodeposited metal to ensure consistent electrodeposition. Tests were conducted in a Lexan cell using a 50-mM phosphate buffer, a Ag/AgCl reference electrode, and a platinum counter electrode (3 cm × 5 mm) with a scan range of 0.2 to −1.2 V and a scan rate of $3\ mV\ s^{-1}$. Consistent electrodeposition was confirmed as all nickel oxide cathodes had similar hydrogen evolution potentials between −0.65 and −0.70 V. The electrodes were subsequently cut to size (3.8 cm diameter disks) and rinsed with deionized water before placing them in the reactors.

2.4. Analysis

Gas production was measured using a respirometer (AER-200, Challenge Technology, AZ). Gas flowing out of the respirometer was collected in sampling gas bags (250 ml capacity, Cali-5 bond, Calibrated Instruments Inc., NY). The composition of the MEC headspace and the gas bags were analyzed using two gas chromatographs (models 8610B and 310, SRI Instruments, CA) equipped with Alltech Molesieve 5A 80/100 stainless steel-tubing columns and thermal conductivity detectors (TCDs). Argon was used as the carrier gas for H_2, O_2, N_2 and CH_4 analysis, and helium was used

as the carrier gas for CO_2 analysis. Voltage across an external resistor (R_{ex} = 10 Ω) was measured using a multimeter (2700, Keithley Instruments, Inc., OH) to calculate current.

Electrochemical experiments were conducted with a potentiostat (PC4/750TM, Echem Analyst, v. 5.5, Gamry Instruments, PA). CV scans were done over three cycles, from 0 to 1 V, at a scan rate of 1 mV s^{-1} on the MEC cells after use. CV scans have been previously performed on whole cell MFCs [22,23] and on separate MEC components [24] for evaluation of biofilms and electron transfer performance. Scanning electron microscopy/energy dispersive X-ray spectroscopy (SEM–EDS) analysis was done at 20 kV (Quanta 200, FEI, OR).

2.5. Calculations

Hydrogen recovery, energy recovery, volumetric density and hydrogen production rates were used to evaluate reactor performance [2]. The theoretical number of hydrogen moles produced ($n_{H_2,COD}$), based on COD removal is:

$$n_{H_2,COD} = \frac{b_{eO_2} v_L \ \Delta COD}{2M_{O_2}} \quad (1)$$

where $b_{eO_2} = 4$ is the number of electrons exchanged per mole of oxygen, $v_L = 32$ ml the volume of liquid in the reactor, M_{O_2} = 32 g mol^{-1} the molecular weight of oxygen, 2 the number of moles of electrons per mole of hydrogen gas, and ΔCOD the change in substrate concentration (g L^{-1}).

The theoretical number of hydrogen moles that can be recovered based on the measured current ($n_{H_2,cat}$) is:

$$n_{H_2,cat} = \frac{\int_{t=0}^{t} I dt}{2F} \quad (2)$$

where $I = V/R_{ex}$ is the current (A) calculated from the voltage across the resistor (10 Ω) and dt is the time interval (1200 s) for data collection.

The overall hydrogen recovery ($r_{H_2,COD}$) is the ratio of hydrogen recovered compared to the maximum theoretical hydrogen produced based on substrate utilization:

$$r_{H_2,COD} = \frac{n_{H_2}}{n_{H_2,COD}} \quad (3)$$

where n_{H_2} is the actual number of hydrogen moles produced. The cathodic hydrogen recovery ($r_{H_2,cat}$) is the fraction of electrons that are recovered as hydrogen gas from the total number of electrons that reach the cathode, or

$$r_{H_2,cat} = \frac{n_{H_2}}{n_{H_2,cat}} \quad (4)$$

The Coulombic efficiency (C_E) is the ratio of electrons recovered as hydrogen gas relative to the total electrons available from substrate consumption, calculated as

$$C_E = \frac{n_{H_2,cat}}{n_{H_2,COD}} = \frac{r_{H_2,COD}}{r_{H_2,cat}} \quad (5)$$

The energy efficiency relative to electrical input (η_E) is the ratio of energy content of hydrogen produced to the input electrical energy:

$$\eta_E = \frac{W_{H_2}}{W_E} = \frac{n_{H_2} \ \Delta H_{H_2}}{\sum_1^n (IE_{ap} \Delta t - I^2 R_{ex} \Delta t)} \quad (6)$$

where W_{H_2} (kJ) is the energy produced by hydrogen, W_E (kJ) the amount of energy added to the circuit by the power source minus the losses across the resistor, ΔH_{H_2} = 285.83 kJ mol^{-1} the energy content of hydrogen based on the heat of combustion and E_{ap} (V) the voltage applied by the power source. The number of moles of substrate consumed during a batch cycle based on COD removal (n_s) is:

$$n_s = \frac{\Delta COD v_L}{M_s} \quad (7)$$

where M_S = 82 g mol^{-1} is the substrate's molecular weight. When using sodium acetate, the molecular weight needs to be multiplied by a conversion factor of 0.78 g COD g^{-1} sodium acetate. The energy efficiency relative to the substrate (η_S) is:

$$\eta_S = \frac{W_{H_2}}{W_S} = \frac{n_{H_2} \ \Delta H_{H_2}}{\Delta H_S n_S} \quad (8)$$

where ΔH_S = 870.28 kJ mol^{-1} is the heat of combustion of the substrate. The overall energy recovery based on both electric and substrate inputs (η_{E+S}) is:

$$\eta_{E+S} = \frac{W_{H_2}}{W_E + W_S} \quad (9)$$

The hydrogen production rate (Q) (m^3 H_2 m^{-3} day^{-1}) was evaluated in terms of current produced per volume of reactor and the gas rate per volume as

$$Q = 3.68 \times 10^{-5} I_V Tr_{H_2,cat} \quad (10)$$

where 3.68×10^{-5} is a constant that includes Faraday's constant, a pressure of 1 atm and unit conversions, I_V (A m^{-3}) is the volumetric current density averaged over a 4-h period of maximum current production and divided by the liquid volume, and T (K) is the temperature.

The Butler–Volmer reaction for hydrogen evolution was used to determine the catalytic performance of the metals, where the reverse current was considered negligible [16,21]. CV scans for the complete MECs were converted to Tafel plots by plotting log I as a function of voltage. The transformed Butler–Volmer equation was used to obtain slopes and y-intercepts via linear regression of the Tafel plots using:

$$\log J = \log J_0 + \frac{\alpha_c n_e F}{2.303RT}(E - E_0) \quad (11)$$

where J (A cm^{-2}) is the current density, J_0 (A cm^{-2}) is the exchange current density, α_c is the cathodic transfer coefficient, n_e is the number of electrons per reaction, E (V) is the working potential and E_0 (V) is the equilibrium potential. The equilibrium potential (E_0) is equal to the hydrogen potential (E_{H_2}):

$$E_{H_2} = 0 + 0.0602 \ \log\left[\frac{1/2H_2}{H^+}\right] = 0 - 0.0602 \ \text{pH} + 0.0301 \log(p_{H_2}) \quad (12)$$

The equilibrium potential $E_0 = E_{H_2} = -0.4458$ V for the experimental conditions presented: T = 30 °C, pH 7 and a partial pressure for hydrogen $p_{H_2} = 0.15$ atm. The hydrogen partial pressure value was the average hydrogen gas composition of all MEC reactors over complete cycles.

3. Results

3.1. Flat cathodes

SS alloys A286 (21.2 ± 2.2 ml) and 304 (19.1 ± 1.1 ml) produced twice as much hydrogen as Ni 201 (9.5 ± 1.6 ml) or SS 316 (9.5 ± 2.6 ml) at an applied voltage of 0.9 V (Fig. 1). Platinum sheet metal produced slightly less hydrogen gas (18.9 ± 5.4 ml) than SS A286 and SS 304. While gas production was consistent over multiple cycles with the SS and Ni materials, gas production with platinum sheet metal decreased with continued use. The total gas production during the first cycle using platinum was 34.5 ± 2.6 ml,

Table 2
Summary of MEC results for different metal cathodes (stainless steel, nickel and platinum) at an applied voltage of 0.9 V.

Metal	$r_{H_2,cat}$ (%)	$r_{H_2,COD}$ (%)	η_E (%)	η_{E+S} (%)	I_V (A m^{-3})	Q (m^3 m^{-3} day^{-1})	H_2 (%)
SS 304	53 ± 1	49 ± 0	90 ± 2	38 ± 1	100 ± 4	0.59 ± 0.01	77 ± 1
SS 316	27 ± 6	25 ± 6	47 ± 10	19 ± 4	116 ± 1	0.35 ± 0.08	55 ± 10
SS 420	43 ± 2	38 ± 1	73 ± 3	30 ± 1	122 ± 10	0.58 ± 0.07	67 ± 2
SS A286	61 ± 3	62 ± 6	107 ± 5	46 ± 3	222 ± 4	1.50 ± 0.04	80 ± 2
Ni 201	27 ± 4	26 ± 3	46 ± 7	20 ± 3	127 ± 8	0.38 ± 0.04	57 ± 3
Ni 400	31 ± 5	31 ± 8	53 ± 9	23 ± 5	116 ± 9	0.41 ± 0.10	62 ± 8
Ni 625	43 ± 9	41 ± 13	75 ± 16	31 ± 8	160 ± 22	0.79 ± 0.27	67 ± 9
Ni HX	40 ± 8	38 ± 7	68 ± 14	29 ± 5	124 ± 14	0.55 ± 0.11	69 ± 4
Pt	47 ± 2	46 ± 4	81 ± 3	35 ± 2	129 ± 7	0.68 ± 0.06	74 ± 2

Table 3
Tafel plots's slopes and *y*-intercepts for MECs with different metal cathodes.

Metal	Low current density		High current density		
	Slope (decade A cm^{-2} V^{-1})	*y*-Intercept (A cm^{-2})	Slope (decade A cm^{-2} V^{-1})	*y*-Intercept (A cm^{-2})	*V*-Intersect (V)
Ni 625	−3.68	−5.37	−0.98	−3.94	−0.54
Ni HX	−3.70	−5.25	−0.91	−3.87	−0.51
Ni 201	−2.38	−4.73	−0.75	−3.74	−0.61
Ni 400	−2.30	−4.84	−0.76	−3.82	−0.67
SS 286	−4.44	−5.34	−0.88	−3.76	−0.45
SS 304	−2.18	−4.53	−0.64	−3.66	−0.56
SS 420	−2.94	−4.85	−0.88	−3.82	−0.49
SS 316	−2.39	−4.61	−0.94	−3.84	−0.53
Pt	−4.31	−5.45	−0.82	−3.75	−0.48

but only 19.2 ± 1.3 ml by the third cycle. This change in gas production resulted in a higher variability of the gas produced with platinum than with the other metals.

The best performing alloys based on MEC recoveries and efficiencies were SS A286, SS 304 and Ni 625 (Table 2) (E_{ap} = 0.9 V). Of these three materials, SS A286 consistently had the best performance for all parameters used to evaluate the MECs ($r_{H_2,cat}$, $r_{H_2,COD}$, η_E, η_{E+S}, I_V, Q, and H_2 content). The hydrogen production rate was significantly higher for SS A286 (Q = 1.5 m^3 m^{-3} day^{-1}) than for any of the other metals, including platinum (Q = 0.68 m^3 m^{-3} day^{-1}). The platinum sheet metal displayed only average performance compared to the other metals, being surpassed by both SS 304 and SS A286 in terms of hydrogen recoveries and energy efficiencies at an applied voltage of 0.9 V.

Overall gas production was reduced for all the metals at a lower applied voltage of 0.6 V (average = 6.8 ± 3.9 ml H_2) compared to 0.9 V (21.3 ± 3.8 ml H_2) as expected from previous studies [3] (Fig. 2). Hydrogen concentrations at 0.6 V were reduced to 17.2 ± 13.2% H_2 (vs. 67.5 ± 8.6% H_2 at 0.9 V), and methane concentrations increased (69.0 ± 13.3% at 0.6 V vs. 23.9 ± 8.3% at 0.9 V). Ni 625 performed better than the other metals in terms of total hydrogen gas production at this lower applied voltage (6.61 ml H_2), but the product gas was mainly methane (47.3% CH_4, 40.8% H_2, 11.9% CO_2). Platinum sheet metal produced only 11.2 ml H_2, with a gas composition of 49.8% CH_4, 35.0% H_2 and 15.1% CO_2. Maximum current densities at 0.9 V were higher for both SS A286 (1.01 ± 0.18 mA cm^{-2}) and Ni 625 (0.73 ± 0.099 mA cm^{-2}) than for the platinum sheet metal (0.59 ± 0.03 mA cm^{-2}) (Fig. 3). At 0.6 V, the difference between current densities of these metals was almost

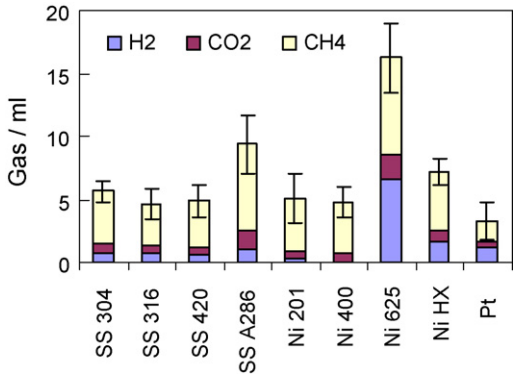

Fig. 2. Gas production of MECs with different stainless steels and nickel cathodes, compared to a platinum disk, at an applied voltage of 0.6 V.

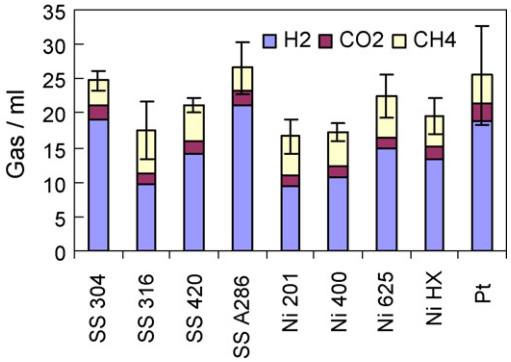

Fig. 1. Gas production of MECs with different stainless steels and nickel cathodes, compared to a platinum disk, at an applied voltage of 0.9 V.

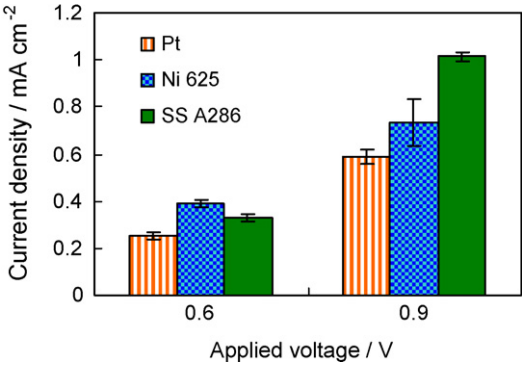

Fig. 3. Current densities for MECs with a platinum disk, Ni 625 and SS A286 cathodes at applied voltages of 0.6 and 0.9 V.

Table 4
Summary of MEC results for metal cathodes with electrodeposited nickel oxide layer, compared to platinum, at an applied voltage of 0.6 V.

Metal	$r_{H_2,cat}$ (%)	$r_{H_2,COD}$ (%)	η_E (%)	η_{E+S} (%)	I_V (A m^{-3})	Q (m^3 m^{-3} day^{-1})	H_2 (%)
SS A286	1.2 ± 0.1	1.1 ± 0.1	3.1 ± 0.1	1.1 ± 0.1	71 ± 3	0.01 ± 0.001	6 ± 1
Ni 625	12 ± 5	11 ± 4	31 ± 13	10 ± 4	86 ± 3	0.1 ± 0.04	35 ± 2
Pt	12 ± 5	4 ± 1	31 ± 12	4 ± 2	55 ± 3	0.08 ± 0.03	36 ± 1
SS A286 + NiO_x	52 ± 4	56 ± 2	137 ± 12	48 ± 3	130 ± 21	0.76 ± 0.16	76 ± 2
Ni 625 + NiO_x	52 ± 9	56 ± 10	137 ± 24	48 ± 9	131 ± 7	0.76 ± 0.15	76 ± 5

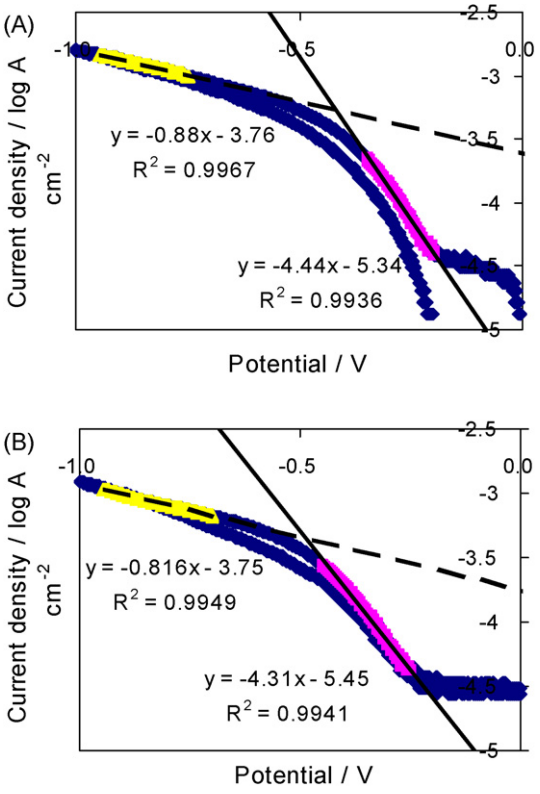

Fig. 4. Tafel plots for MECs for (A) stainless steel 286 alloy and (B) platinum metal cathodes.

non-existent (0.25 ± 0.014 to 0.39 ± 0.014 mA cm^{-2}). Therefore, a higher applied voltage was needed to properly differentiate these metal surfaces.

The performance of the metal alloys for use as cathodes in MECs was evaluated on the basis of the slopes and *y*-intercepts from Tafel plots (Table 3). The Tafel plots for SS A286 and platinum are shown as typical examples in Fig. 4, with two linear regions: one at high current densities (solid line) and one at low current densities (dashed line). The larger Tafel slopes and *y*-intercepts indicate better catalytic performance. The Tafel slope is a function of the transfer coefficient α_c and the number of electrons n_e transferred during the reaction. The *y*-intercept is controlled by the exchange current density J_0. The best cathodes based on Tafel slopes and *y*-intercepts were SS 286, Ni 625, Ni HX and platinum sheet metal, with slopes ranging from 3.68 to 4.31 decade A cm^{-2} V^{-1} and *y*-intercepts of 5.25–5.45 A cm^{-2} at low current densities. *V*-intersect is the voltage at which the linear regressions intersect. Ideally, the MEC should operate at a higher current density for a given overpotential. SS 286 has the lowest *V*-intersect (0.45 V) of all the metals tested. The ranking of the metal alloys based on electrochemical results thus confirms the same relative performance of the materials observed in MEC tests.

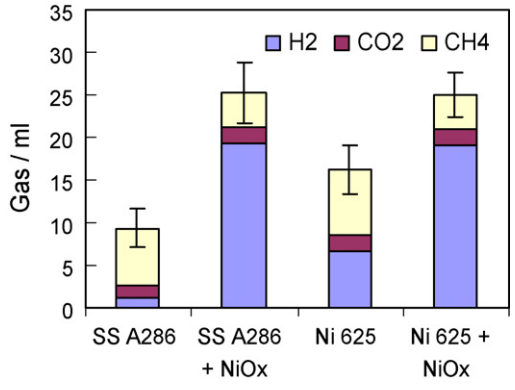

Fig. 5. Gas production of MECs with and without electrodeposited nickel oxide layers on SS A286 and Ni 625 at an applied voltage of 0.6 V.

3.2. Particles on carbon cloth cathodes compared to metal sheet cathodes

The performance of the platinum sheet metal was compared to the higher surface area platinum particle catalyst bound on carbon cloth usually used in MEC studies. Current densities produced by the platinum sheet metal cathode at an applied voltage of 0.9 V (0.59 ± 0.03 mA cm^{-2}) were similar to the current densities achieved by the platinum particle bound on carbon cloth at an applied voltage of 0.6 V (0.56 ± 0.03 mA cm^{-2}). As expected, the MECs performed better with platinum particle catalyst than with the platinum metal sheet as similar current densities were achieved at lower applied voltages.

3.3. Nickel oxide cathodes

The performance of the best MEC materials (SS A286 and Ni 625) was further improved by electrodepositing a nickel oxide layer on the surface of the sheet metal. Gas production increased from 9.4 to 25 ml for SS A286 and from 16.2 to 25 ml for Ni 625 (Fig. 5) at an applied voltage of 0.6 V. Methane gas production was reduced from 6.8 to 4.1 ml for SS A286 and from 7.7 to 4.2 ml for Ni 625. Hydrogen production and recoveries were 4–40 times higher than the original values without the metal oxide (Table 4). Both nickel oxide modified metals reached similar hydrogen production and recovery values, suggesting the sheet metal was less of a factor than the metal oxide surface for performance. For example, energy recovery based on electrical input (η_E) increased from 3.1% (SS A286) and 31% (Ni 625) to 137% for both SS A286 and Ni 625 plus nickel oxide. Volumetric hydrogen production rates (*Q*) also improved from 0.01 (SS A286) and 0.1 (Ni 625) to 0.76 m^3 H_2 m^{-3} day^{-1} for both nickel oxide modified metals. In comparison, platinum sheet metal performance at applied 0.6 V was similar to the performance of metals without the nickel oxide layer (Table 4): low recoveries (η_E = 31%, η_{E+S} = 4%), low gas production (*Q* = 0.08 m^3 H_2 m^{-3} day^{-1}) and low hydrogen content (H_2 = 36%).

Stability of the MECs with nickel oxide cathodes was examined by running the reactors for 15 days (Fig. 6). The initial high gas production and current densities decreased over the first few cycles. Current appeared to stabilize after the first three cycles, while

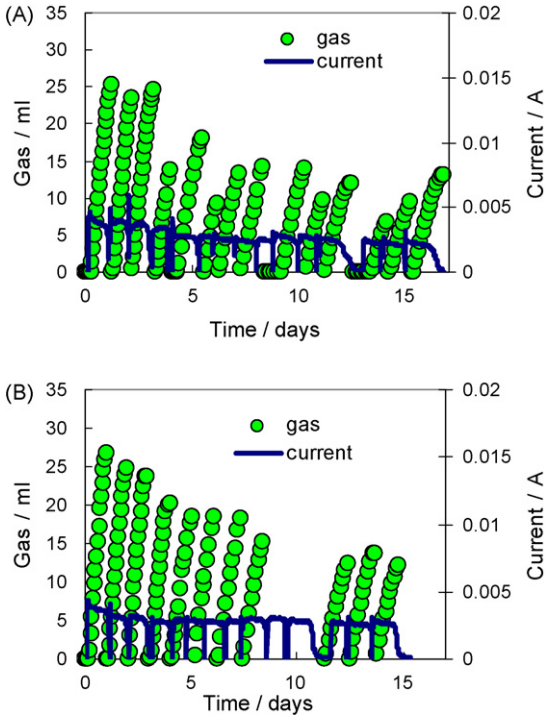

Fig. 6. Total gas and current production versus time with (A) Ni 625 + NiO_x and (B) SS A286 + NiO_x cathodes.

gas production stabilized after seven cycles. The initial decrease in performance was confirmed through changes in the Tafel plot parameters (Table 5). There was a 30% decrease in Tafel slope values between day 5 and day 15 (1.87 to 1.29 decade A cm^{-2} V^{-1} for Ni 625 + NiO_x; 1.54 to 1.04 decade A cm^{-2} V^{-1} for SS 286 + NiO_x), and a slight decrease in the *y*-intercept values (4.10 to 4.06 A cm^{-2} for Ni 625 + NiO_x; 3.90 to 3.82 A cm^{-2} for SS A286 + NiO_x).

Table 5
Tafel plots's slope and *y*-intercepts for MECs with and without nickel oxide electrodeposited on Ni 625 and SS 286 alloys.

Metal	Day #	Slope (decade A cm^{-2} V^{-1})	*y*-Intercept (A cm^{-2})
Ni 625 + NiOx	5	−1.87	−4.10
Ni 625 + NiO_x	15	−1.29	−4.06
SS 286 + NiO_x	5	−1.54	−3.90
SS 286 + NiO_x	15	−1.04	−3.82

The surfaces of the metal oxides deposited on SS A286 observed using SEM (Fig. 7) indicate finer structures before use, compared to dull structures 8 days after use. The metal composition by SEM–EDS (Table 6) shows 15 times higher weight percent values for nickel compared to oxygen on the "before" electrodeposited sample, which is equivalent to 4.2 atoms of nickel per atom of oxygen. The SEM–EDS analysis also shows small metal composition differences in the non-modified SS A286 and Ni 625 alloys before and after use, but large differences in the nickel oxide on SS A286 cathode. The most important finding was the decrease in nickel content (from 52.4 to 21.8 wt%), suggesting that some of the oxide layer was removed from the surface. There were increases in chromium (from 7.98 to 11.3 wt%), oxygen (from 3.5 to 8.5 wt%), and iron (from 31.2 to 43.9 wt%). The increase in chromium and iron suggests that the stainless steel metal contributed 40% more to the "after" composition compared to the "before" composition. Carbon, phosphorus, sodium and sulfur also increased, perhaps as a result of exposure to buffer and bacteria.

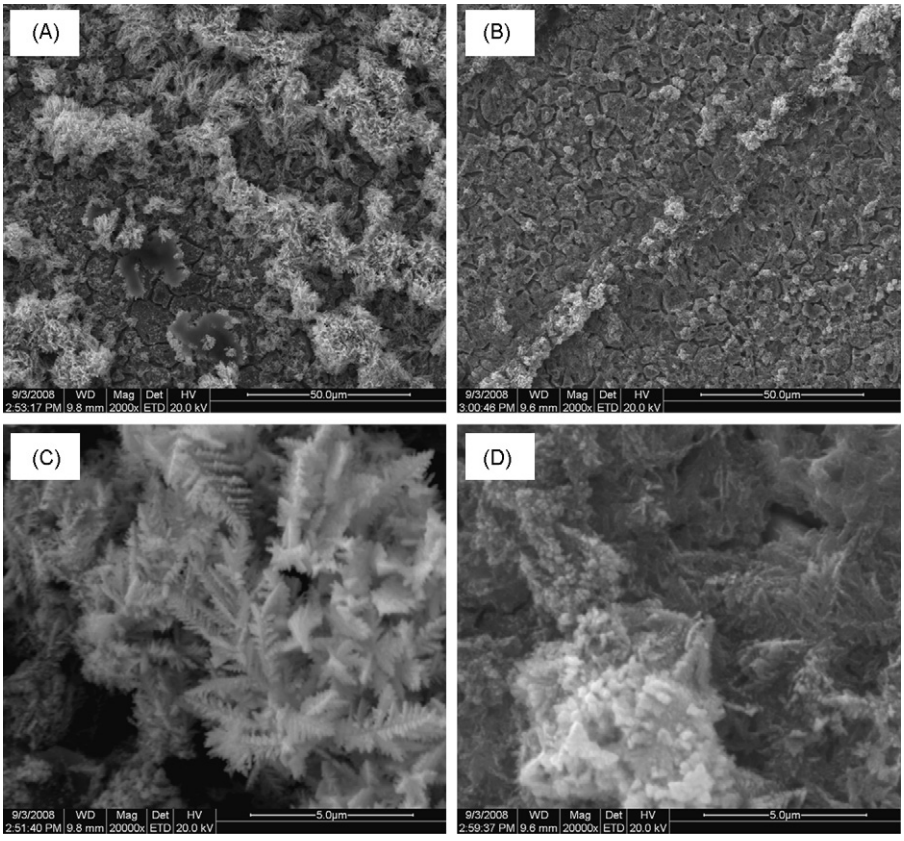

Fig. 7. SEM images of SS A286 + NiO_x (A and C) before and (B and D) after 8-day use as cathode in MEC. (A) and (B) are at 2000× magnification and (C) and (D) are at 20,000× magnification.

Table 6
Metal composition by SEM–EDS before and after 8 days of use in MEC as cathode.

Metal	Ni 625		SS A286		SS A286 + NiO_x	
	Before (wt%)	After (wt%)	Before (wt%)	After (wt%)	Before (wt%)	After (wt%)
C	5.56	7.36	3.58	7.70	2.98	5.17
O	1.76	2.80			3.50	8.54
Cr	17.22	16.10	14.80	14.10	7.98	11.32
Fe	6.04	5.90	58.70	53.70	31.20	43.95
Ni	61.90	60.00	19.50	17.90	52.40	21.80
Mo	7.49	7.85	1.22	1.41		
Ti			2.24	1.77	1.20	1.20
P						1.00
Na						1.54
S						4.41

4. Discussion

4.1. Cathode efficiency

Platinum has been assumed to be the most efficient catalyst for electrohydrogenesis in MECs. The results obtained here, however, show that the performance of platinum can be surpassed by certain stainless steel and nickel alloys. In all cases, for example, SS A286 showed better performance than platinum and the other alloys evaluated in terms of hydrogen gas production, total gas production, cathodic hydrogen recoveries ($r_{H_2,cat}$) and energy recoveries (η_E, η_{E+S}). Furthermore, the volumetric hydrogen production rate (Q) for SS A286 was 4.3 times higher than the SS 316, and 2.2 times better than platinum sheet metal disk. Tafel slopes and intercepts confirmed the superior performance of SS A286 and the general ranking of the other alloys evaluated in MEC tests.

Based on the composition of the SS A286 compared to the other materials, the nickel/iron composition of this alloy appears to be an important factor in their hydrogen evolution performance. The SS A286 has the most nickel (24–27%) compared to the other stainless steel alloys tested, and Ni 625 (the best performing nickel alloy) had the second highest iron content (2.5%) of the nickel alloys tested.

The decrease of platinum activity with use (Fig. 1) can be due to metal poisoning, resulting in a reduction in chemical activity and the number of active sites for hydrogen production. Several chemicals can poison the catalytic activity of platinum, such those containing sulfur, hexamethyldisiloxane (HDMS), silicon, nitric oxide and carbon monoxide [25,26]. In an MEC environment, sulfur and nitrogen are present and could be contributing to platinum poisoning. This poisoning is not observed in the powder platinum catalyst applied with Nafion™ on carbon cloth [1,2,17], perhaps due to the protection provided by the Nafion™.

There was substantial methane production at the lower applied voltage, but the amount of methane produced decreased in tests at the higher applied voltage. The increased methane production rates at the lower voltage can be explained by the longer cycle times (36–80 h) at 0.6 V, compared to shorter cycle times (~24 h) at 0.9 V. The metal cathode with the shortest cycle time at applied 0.6 V (Ni 625; 36 h) also had the highest gas production rate and hydrogen concentration. Long cycle times facilitate growth of methanogens. These microorganisms convert organic matter to methane, but they grow slowly. Methanogens decrease hydrogen gas levels by competing for organic matter in the media (acetate), and scavenging existing hydrogen gas to form methane [27]. This increased methane generation concentrations at longer cycle times has also been observed using platinum on carbon cloth cathodes in MEC tests [3].

The use of nickel oxides on the cathode is a promising method for increasing MEC performance, but the material must be stabilized. When a nickel oxide layer was applied to the cathode by electrodeposition, current densities, total hydrogen gas production, cathodic recoveries, energy efficiencies, and hydrogen production rates improved by a factor of four. It was also found that the MEC provided good performance, even at the lower applied voltage of 0.6 V. The use of a lower voltage significantly improved the process energy efficiency based on energy input, for example, from η_E = 3.1% (SS A286) and η_E = 31% (Ni 625) to η_E = 137% (nickel oxide on either metal surface). However, performance of the metal oxides showed an initial decrease but stabilized with repeated cycles, and thus additional work is needed to maintain the performance of these materials over time. Also, future work should address to what extent improvement in initial performance was due to a surface area, and if other metals used as a base for the metal oxide would be a factor in performance.

4.2. Cathode costs

The cost of the metal sheets used here represents a one to two order of magnitude decrease in costs compared to traditional Pt and carbon cloth cathodes. The cost of the sheet metals varied from \$73 m^{-2} (SS 304) to \$370 m^{-2} (Ni 625) (www.mcmaster.com). A typical platinum particle catalyst on a carbon cloth cathode costs *ca.* \$2,300 m^{-2} based on \$850 m^{-2} for the carbon cloth (BASF Fuel Cell, Inc., NJ), \$700 m^{-2} for the platinum particle catalyst (BASF Fuel Cell, Inc., NJ), and \$750 m^{-2} for the binder (Nafion™, Sigma–Aldrich, MO). To put these costs in perspective, for an MEC with 100 m^2 of surface area per cubic meter of reactor volume (100 m^2 m^{-3}), the cost would be \$730 for a sheet metal cathode compared to \$200,300 for a typical platinum catalyst on carbon cloth. This cost could be further decreased by using this metal in different surface configurations and thicknesses.

There are additional costs to deposit nickel oxide onto the sheet metal. The cost to treat 100 m^2 of cathode is estimated to be \$240 (1 cm^3 of solution per 1 cm^2 of cathode area) for \$0.236 L^{-1} of solution (0.012 M $NiSO_4$ at \$0.196 L^{-1}, 20 mM $(NH_4)_2SO_4$ at \$0.031 L^{-1}, H_2SO_4 at \$0.01 L^{-1}) (www.sial.com). The electrical requirement needed for the process is negligible (<\$0.01 m^{-2} at \$0.11 kW h^{-1}) (www.eia.doe.gov/cneaf/electricity/epm/tablees1a.html) as the required voltage is only applied for 30 s. Therefore, the addition of a nickel oxide layer on the cathode is minor compared to the cost of the support material.

5. Conclusions

Performance of stainless steel and nickel alloys was similar or better than platinum sheet metal when used as cathodes in MECs. Stainless steel A286 showed the best performance of all the alloys tested at an applied potential of 0.9 V. Lower applied voltages resulted in long cycle times and low hydrogen production rates. A nickel oxide layer electrodeposited on the metal surfaces improved their catalytic performance by at least a factor of four. Mechanical long term stability of the nickel oxide layer needs to be improved

by evaluating combinations of different supports and catalysts, and possibly binding agents. The nickel oxide layer and sheet metal support are relatively inexpensive and good candidates for large scale applications.

Acknowledgements

The authors thank S. Cheng, D. Call, E. Lalaurette and D. Jones for assistance with MEC experiments, and J.M. Perez and W.A. Lloyd for their advice and insight. This research was supported in part by the Global Research Partnership (GRP) from KAUST University, the General Electric First-Year Faculty for the Future Fellowship and the Arthur and Elizabeth Rose Memorial Fellowship, and Air Products and Chemicals, Inc.

References

[1] B.E. Logan, Microbial Fuel Cells, John Wiley & Sons, Inc., Hoboken, NJ, 2008, pp. 125–144.
[2] B.E. Logan, D. Call, S. Cheng, H.V.M. Hamelers, T.H.J.A. Sleutels, A. Jeremiasse, R.A. Rozendal, Environ. Sci. Technol. 42 (2008) 8630–8640.
[3] D. Call, B.E. Logan, Environ. Sci. Technol. 42 (2008) 3401–3406.
[4] J. Ditzig, H. Liu, B.E. Logan, Int. J. Hydrogen Energy 32 (2007) 2296–2304.
[5] S. Cheng, B.E. Logan, PNAS 104 (2007) 18871–18873.
[6] H. Liu, S. Grot, B.E. Logan, Environ. Sci. Technol. 39 (2005) 4317–4320.
[7] W. Liu, A. Wang, N. Ren, X. Zhao, L. Liu, Z. Yu, D. Lee, Energy Fuels 22 (2008) 159–163.
[8] R.A. Rozendal, H.V.M. Hamelers, G.J.W. Euverink, S.J. Metz, C.J.N. Buisman, Int. J. Hydrogen Energy 31 (2006) 1632–1640.
[9] R.A. Rozendal, H.V.M. Hamelers, R.J. Molenkamp, C.J.N. Buisman, Water Res. 41 (2007) 1984–1994.
[10] B. Tartakovsky, M.-F. Manuel, V. Neburchilov, H. Wang, S.R. Guiot, J. Power Sources 182 (2008) 291–297.
[11] R.A. Rozendal, A.W. Jeremiasse, H.V.M. Hamelers, C.J.N. Buisman, Environ. Sci. Technol. 42 (2008) 629–634.
[12] A.M. Couper, D. Pletcher, F.C. Walsh, Chem. Rev. 90 (1990) 837–865.
[13] J.M. Olivares-Ramirez, M.L. Campos-Cornelio, J. Uribe Godinez, E. Borja-Arco, R.H. Castellanos, Int. J. Hydrogen Energy 32 (2007) 3170–3173.
[14] D. Marcelo, A. Dell'Era, Int. J. Hydrogen Energy 33 (2008) 3041–3044.
[15] J.R.C. Salgado, M.H.S. Andrade, J.C.P. Silva, J. Tonholo, Electrochem. Acta 47 (2002) 1997–2004.
[16] M.D. Merrill, Water Electrolysis at the Thermodynamic Limit. Doctoral Dissertation, Florida State University, 2007, pp. 20–57.
[17] B.E. Logan, S. Cheng, V. Watson, G. Estadt, Environ. Sci. Technol. 41 (2007) 3341–3346.
[18] S. Cheng, B.E. Logan, Electrochem. Commun. 9 (2006) 492–496.
[19] H. Liu, B.E. Logan, Environ. Sci. Technol. 38 (2004) 2281–2285.
[20] S. Cheng, H. Liu, B.E. Logan, Environ. Sci. Technol. 40 (2006) 364–369.
[21] M.D. Merrill, R.C. Dougherty, J. Phys. Chem. 112 (2008) 3655–3666.
[22] E. Marsili, J.B. Rollefson, D.B. Baron, R.M. Holzalski, D.R. Bond, Appl. Environ. Microbiol. 74 (2008) 7329–7337.
[23] L. Zhang, S. Zhou, L. Zhuang, W. Li, J. Zhang, N. Lu, L. Deng, Electrochem. Commun. 10 (2008) 1641–1643.
[24] S. Cheng, B.E. Logan, Water Sci. Technol. 58 (2008) 853–857.
[25] D.U. Hong, C. Han, S.H. Park, I. Kim, J. Gwak, S. Han, H.J. Kim, Curr. Appl. Phys. 9 (2009) 172–178.
[26] K. Kwon, D.Y. Yoo, J.O. Park, J. Power Sources 185 (2008) 202–206.
[27] R.A. Rozendal, H.V.M. Hamelers, K. Rabaey, J. Keller, C.J.N. Buisman, Trends Biotechnol. 26 (2008) 450–459.